Global Journal of Science Frontier Research: I
Interdisciplinary
Volume 17 Issue 2 Version 1.0 Year 2017
Type: Double Blind Peer Reviewed International Research Journal
Publisher: Global Journals Inc. (USA)
Online ISSN: 2249-4626 & Print ISSN: 0975-5896

Underground Storage of Natural Gas in Hydrate State: Primary Injection Stage

By E. A. Bondarev, I. I. Rozhin, V. V. Popov & K. K. Argunova
Ammosov North-Eastern Federal University

Abstract- The paper is devoted to simulation of the initial stage of natural gas hydrate underground storage: gas injection into aquifer just below permafrost rocks. It is based on the mathematical model of multiphase non-isothermal real gas and water flow in porous media. The model takes into account the transformation of gas and water into hydrate at certain temperature which depends on gas flow pressure. The dynamics of hydrate and water saturation as well as the pressure and temperature fields in a reservoir with given porosity, permeability and initial values of pressure, temperature and water saturation have been studied. An implicit finite-difference scheme is used to approximate the original boundary-value problem. The finite-difference equations have been solved using simple iteration and sweeping algorithms. Several examples of calculations corresponding to real cases are given. Calculations have revealed that the final result strongly depends on the combination of porosity and permeability of a reservoir.

Keywords: *permafrost, underground storage, natural gas, hydrate formation, mathematical modeling.*

GJSFR-I Classification: *FOR Code: 850499*

Strictly as per the compliance and regulations of:

Underground Storage of Natural Gas in Hydrate State: Primary Injection Stage

E. A. Bondarev [α], I. I. Rozhin [σ], V. V. Popov [ρ] & K. K. Argunova [ω]

Abstract- The paper is devoted to simulation of the initial stage of natural gas hydrate underground storage: gas injection into aquifer just below permafrost rocks. It is based on the mathematical model of multiphase non-isothermal real gas and water flow in porous media. The model takes into account the transformation of gas and water into hydrate at certain temperature which depends on gas flow pressure. The dynamics of hydrate and water saturation as well as the pressure and temperature fields in a reservoir with given porosity, permeability and initial values of pressure, temperature and water saturation have been studied. An implicit finite-difference scheme is used to approximate the original boundary-value problem. The finite-difference equations have been solved using simple iteration and sweeping algorithms. Several examples of calculations corresponding to real cases are given. Calculations have revealed that the final result strongly depends on the combination of porosity and permeability of a reservoir.

Keywords: permafrost, underground storage, natural gas, hydrate formation, mathematical modeling.

I. Introduction

Nowadays underground gas storages are built in the depleted gas reservoirs or aquifers situated near gas pipelines or large centers of gas consumption. Along with the peak-shaving storages, they are used to meet load variations, that is, gas is injected into storage during periods of low demand and is withdrawn during periods of peak one, which is especially important for the Northern regions where they can be used as distinctive accumulators of natural gas.

One of the alternatives to common gas storages would be those of hydrates compounds formed when natural gas is injected into porous reservoirs under certain thermodynamic conditions (at specific temperature – pressure relations controlled by the gas composition). Subpermafrost aquifers in the areas of continuous permafrost act readily as such reservoirs. For example, in Central Yakutia, they can occur directly beneath the permafrost base at depths of 500-600 m [*Balobaev et al., 2003*], with permeability ranging between10^{-12} and 10^{-14} m^2.

In [*Duchkov et al., 2009*] it is shown that carbon dioxide sequestration in the subpermafrost horizons is possible through CO_2 injections into reservoirs located beneath the carbon dioxide hydrate stability zone. Major advantages of this method consist in greater compactness and stability of the repository, given that gas in a solid state occupies a considerably smaller volume versus its being in free state at equal temperature and pressure, and that during gas transition into the hydrate state all free reservoir water becomes bound. The already known method of natural gas hydrate storage consists of hydrate formation in special aboveground tanks, analogous to liquefied gas storages.

In the paper [*Bondarev et al, 2015*] conceptual possibility of natural gas underground storage in hydrate state was proved via mathematical modeling of gas injection into water saturated reservoir at shallow depths corresponding to the permafrost base in the central part of Eastern Siberia. Gas injection time was limited to 10 days. The model takes into account key physical features of the process: real gas properties, Joule-Thomson effect, simultaneous flow of water–gas mixture, and mass transfer between gas, water and hydrate. Here the authors extend time of gas injection up to 100 days, which corresponds to real period of lower gas consumption during the summer.

II. Problem Formulation

To assess the concept of storing natural gas occurring in hydrate state consider a standard axisymmetric problem of gas injection into a horizontal aquifer, with impermeable and thermally insulated top and bottom, through a single well. Let us assume that gas flows in the reservoir initially saturated with water. Porous matrix is considered rigid, gas is only in the gaseous/hydrate state, whereas water – only in the liquid/hydrate states, that is neither ice nor vapor are formed.

In [*Bondarev et al., 2009*] it was shown that, the role of thermal conductivity is negligible versus forced convection in overall heat transfer balance and, therefore, the heat conductivity term in the energy equation is set to zero. Then, in the frame of multiphase flow mechanics [*Bondarev et al., 1976; Basniyev et al., 1986*] and subject to the generalized Darcy's law, the

Author α: Institute of Oil and Gas Problems, SB RAS, 1 Oktyabrskaya str., Yakutsk, 677980, Russia. e-mail: bondarev@ipng.ysn.ru
Author σ: Ammosov North-Eastern Federal University, 58 Belinskogo str., Yakutsk, 677000, Russia.

energy equation in cylindrical coordinates takes the following form:

$$(\rho c)_e \frac{\partial T}{\partial t} - mq\rho_h \frac{\partial \nu}{\partial t} - m(1-\nu-\sigma)\left(1+\frac{T}{z}\frac{\partial z}{\partial T}\right)\frac{\partial p}{\partial t} -$$

$$-k(1-\nu)\left(\rho_w c_w \frac{f_w}{\mu_w} + \rho_g c_g \frac{f_g}{\mu_g}\right)\frac{\partial p}{\partial r}\frac{\partial T}{\partial r} +$$

$$+k(1-\nu)\rho_g c_g \frac{f_g}{\mu_g}\frac{RT^2}{c_p p}\frac{\partial z}{\partial T}\left(\frac{\partial p}{\partial r}\right)^2 = 0, \quad (1)$$

where $(\rho c)_e = (1-m)\rho_s c_s + m(1-\nu-\sigma)\rho_g c_g + m\nu\rho_h c_h + m\sigma\rho_w c_w$ – is effective value of specific volume heat capacity of porous medium saturated with gas, hydrate and water.

The equations of gas and water filtration are to be written down in these same coordinates:

$$m\frac{\partial}{\partial t}\left((1-\nu-\sigma)\frac{p}{zT}\right) =$$

$$= \frac{1}{r}\frac{\partial}{\partial r}\left(r\frac{k(1-\nu)f_g}{\mu_g}\frac{p}{zT}\frac{\partial p}{\partial r}\right) - m\rho_h \varepsilon R\frac{\partial \nu}{\partial t}, \quad (2)$$

$$m\frac{\partial \sigma}{\partial t} = \frac{1}{r}\frac{\partial}{\partial r}\left(r\frac{k(1-\nu)f_w}{\mu_w}\frac{\partial p}{\partial r}\right) - m(1-\varepsilon)\frac{\rho_h}{\rho_w}\frac{\partial \nu}{\partial t}. \quad (3)$$

Here and elsewhere the following notations are used: c –specific heat capacity; f –relative permeability; k –absolute permeability; m –porosity; p –pressure; q –latent heat of "hydrate–gas+water" phase change; R –gas constant; r –space coordinate; r_b –well radius; r_k –external boundary radius; T – temperature; t –time; z –gas compressibility function; ε –gas content per hydrate unit volume; μ –dynamic viscosity; ρ –density; σ –water saturation; ν –hydrate saturation. The lower indices $g, h, s, w, 0$ stand for gas, hydrate, solid matrix, water and reference state, respectively.

To find a single-valued of the (1) - (3) set, initial and boundary conditions should be formulated. Constant values of pressure, temperature, hydrate saturation and water content have been chosen as initial conditions:

$$p(r,0) = p_0,\ T(r,0) = T_0,\ \nu(r,0) = \nu_0,\ \sigma(r,0) = \sigma_0 \quad (4)$$

At gas injection point (bottom hole), the following conditions are set:
constant temperature

$$T(r_b, t) = T_b \quad (5)$$

and bottom hole gas pressure

$$p(r_b, t) = p_b(t), \quad (6)$$

or its volume flow rate (modified to normal physical conditions)

$$2\pi r_b H \frac{\rho_g}{\rho_n}\frac{k(1-\nu)f_g}{\mu_g}\frac{\partial p(r_b,t)}{\partial r} = -Q, \quad (7)$$

where H – reservoir thickness; ρ_n – gas density at $p_n = 101325$ Pa and $T_n = 273.15$ K.

Instead of impermeability condition at reservoir boundary used in [*Bondarev et al, 2015*] here the possibility of water flow outside storage boundary is stated

$$-\frac{\partial p(r_k,t)}{\partial r} = \frac{f_w(p(r_k,t)-p_0)}{r_k \ln(r_{out}/r_k)}. \quad (8)$$

where r_{out} – radial distance of hydrodynamic influence.
Equations of the problem are closed by:

1) The relations for gas and water relative permeabilities [*Charnyi, 1963*]

$$f_g(\sigma) = \begin{cases}\left(1-\frac{\sigma}{0.9}\right)^{3.5}(1+3\sigma), & 0 \le \sigma < 0.9;\\ 0, & \sigma \ge 0.9\end{cases} \quad (9)$$

$$f_w(\sigma) = \begin{cases}\left(\frac{\sigma-0.2}{0.8}\right)^{3.5}, & 0.2 < \sigma \le 1;\\ 0, & 0 \le \sigma \le 0.2\end{cases} \quad (10)$$

2) The gas-hydrate–water thermodynamic equilibrium condition

$$T = \alpha_1 \ln p + \alpha_2, \quad (11)$$

where α_1, α_2 – empirical constants determined through experimental data or calculated for gas of a given composition, on the basis of methods described in [*Istomin and Kvon, 2004; Sloan and Koh, 2008*];

3) Equation of state for real gas

$$\rho_g = p/zRT, \quad (12)$$

where dependent on pressure and temperature gas compressibility function is approximated by the Latonov–Gurevich empirical equation [*Latonov and Gurevich, 1969*]:

$$z = (0.17376\ln(T/T_c) + 0.73)^{p/p_c} + 0.1\,p/p_c.$$

Critical parameters of natural gas are determined according to its composition by the Kay's Rule (for non-ideal gas mixtures) [*Kay, 1936*]:

$$p_c = \sum_{i=1}^{n} y_i p_{ci},\ T_c = \sum_{i=1}^{n} y_i T_{ci},$$

where p_{ci}, T_{ci}, y_i – are critical pressure and temperature and molar fraction of the i-th component of natural gas.

The method of finite differences is applied to solve the problem (1) - (12). Here with the original equations, boundary and initial conditions are replaced by their mesh analogues [*Bondarev et al, 2009*], whereas the proposed by [*Vasiliev et al., 2000; Bondarev and Popov, 2002*] algorithm for implementation of simple iterations method was applied for solving the corresponding system of algebraic equations at each time step.

III. Numerical Implementation of the Model and its Algorithm

To solve the initial value problem (1)-(12), replace $p(r_i,t_j)=p_i^j$, $T(r_i,t_j)=T_i^j$, $\nu(r_i,t_j)=\nu_i^j$ and $\sigma(r_i,t_j)=\sigma_i^j$ with numerical analogues in the space-time mesh points we approximate equations (1)-(8) by purely implicit absolutely stable difference scheme:

$$(\rho c)_{e,i}\frac{T_i^j-T_i^{j-1}}{\tau}-mq\rho_h\frac{\nu_i^j-\nu_i^{j-1}}{\tau}-m\left(1-\nu_i^j-\sigma_i^j\right)\times$$

$$\times\left(1+\frac{T_i^j}{z_i^j}\left(\frac{\partial z}{\partial T}\right)_i^j\right)\frac{p_i^j-p_i^{j-1}}{\tau_n}=k\left(1-\nu_i^j\right)\times$$

$$\times\left(\rho_w\frac{c_w f_{w,i}}{\mu_w}+\frac{p_i^j}{z_i^j RT_i^j}\frac{c_g f_{g,i}}{\mu_g}\right)\frac{p_{i+1}^j-p_i^j}{h_{i+1}}\frac{T_{i+1}^j-T_i^j}{h_{i+1}}-$$

$$-\frac{k\left(1-\nu_i^j\right)f_{g,i}}{\mu_g}\frac{T_i^j}{z_i^j}\left(\frac{\partial z}{\partial T}\right)_i^j\left(\frac{p_{i+1}^j-p_i^j}{h_{i+1}}\right)^2,$$

$$i=\overline{1,n-1},\ \ j>0; \tag{13}$$

$$m\left(\left(1-\nu_i^j-\sigma_i^j\right)\frac{p_i^j}{z_i^j T_i^j}-\left(1-\nu_i^{j-1}-\sigma_i^{j-1}\right)\frac{p_i^{j-1}}{z_i^{j-1}T_i^{j-1}}\right)\times$$

$$\times\frac{\hbar_i r_i}{\tau}+m\rho_h\varepsilon R\frac{\nu_i^j-\nu_i^{j-1}}{\tau}\hbar_i r_i=$$

$$=\left(r\frac{k\left(1-\nu\right)f_g}{\mu_g}\frac{p}{zT}\right)_{i+1/2}^j\frac{p_{i+1}^j-p_i^j}{h_{i+1}}-$$

$$-\left(r\frac{k\left(1-\nu\right)f_g}{\mu_g}\frac{p}{zT}\right)_{i-1/2}^j\frac{p_i^j-p_{i-1}^j}{h_i},\ \ i=\overline{1,n-1};\tag{14}$$

$$m\frac{\sigma_i^j-\sigma_i^{j-1}}{\tau}\hbar_i r_i+m\left(1-\varepsilon\right)\frac{\rho_h}{\rho_w}\frac{\nu_i^j-\nu_i^{j-1}}{\tau}\hbar_i r_i=$$

$$=\left(r\frac{k\left(1-\nu\right)f_w}{\mu_w}\right)_{i+1/2}^j\frac{p_{i+1}^j-p_i^j}{h_{i+1}}-$$

$$-\left(r\frac{k\left(1-\nu\right)f_w}{\mu_w}\right)_{i-1/2}^j\frac{p_i^j-p_{i-1}^j}{h_i},\ \ i=\overline{1,n-1},\ \ j>0;\tag{15}$$

$$p_i^0=p_0,\ \ T_i^0=T_0,\ \ \nu_i^0=\nu_0,\ \ \sigma_i^0=\sigma_0,\ \ i=\overline{0,n};\tag{16}$$

$$T_0^j=T_b,\ \ j>0;\tag{17}$$

$$p_0^j=p_b \text{ or}$$

$$2\pi r_b H\frac{p_0^j}{z_0^j RT_0^j}\frac{k\left(1-\nu_0^j\right)f_{g,0}}{\rho_n\mu_g}\frac{p_1^j-p_0^j}{h_1}=-Q,\ \ j>0;\tag{18}$$

where τ is a constant step of time mesh $\overline{\omega}_\tau=\left\{t_j=j\cdot\tau,\ j=\overline{0,J}\right\}$; h_i is a constant step of radial mesh $\overline{\omega}_h=\left\{r_{i+1}=r_i+h_{i+1},\ h_{i+1}=\left(r_k-r_b\right)/n,\ i=\overline{0,n-1};\right.$ $\left.r_0=r_b,\ h_0=0\right\}$; and $\hbar_i=\left(h_i+h_{i+1}\right)/2$ is a step of flow mesh.

In the finite-difference form, the right-hand side boundary condition is written with a first order approximation:

$$-\frac{p_n^j-p_{n-1}^j}{h_n}=\frac{f_{w,n}\left(p_n^j-p_0\right)}{r_k\ln\left(r_{out}/r_k\right)}\tag{19}$$

To solve the set of non-linear algebraic equations (13) - (19) one can use the following implementation algorithm of simple iteration method at each time step. First, using (13), we exclude the expression $\left(\nu_i^j-\nu_i^{j-1}\right)/\tau$ from (14), replacing at the same time each and every T_i^j with $\alpha_1\ln p_i^j+\alpha_2$. In the resulting equation, the discrete analogue of time temperature derivative is replaced with the finite-difference analogue of time pressure derivative. The follow-up algorithm involves the following operations as to:

1. Give initial value of the iterations counter $s=0$ and initial approximations of the of pressure, temperature, water and hydrate saturations distributions equal to their corresponding values on the lower time step:

$$\overset{s}{p}_i=p_i^{j-1},\ \overset{s}{T}_i=T_i^{j-1},\ \overset{s}{\nu}_i=\nu_i^{j-1},\ \overset{s}{\sigma}_i=\sigma_i^{j-1},\ i=\overline{0,n}.$$

2. Increase an iterations counter by one unit and then multiply the equation (15) by $p_i^j/\left(z_i^j T_i^j\right)$ and sum it up with equation (14). The resulting equation is solved by the stream sweeping method for calculating the pressure distribution $\overset{s}{p}_i$, $i=\overline{0,n}$.

3. Beginning from the left-hand side ($i = 0$),for all $\overset{s}{\sigma}_i > 0$ the distribution of hydrate saturation $\overset{s}{\nu}_i$, is obtained from equation (13), while the temperature distribution resulted from the three-phase hydrate-gas-water equilibrium $\overset{s}{T}_i = \alpha_1 \ln \overset{s}{p}_i + \alpha_2$, $i = \overline{0, n}$. In case of $\overset{s}{\sigma}_i = 0$ the equation (13) instantly gives the temperature distribution $\overset{s}{T}_i$.
4. Water saturation distribution $\overset{s}{\sigma}_i$, is derived from equation (15). The calculations also start from the left-hand side.
5. Steps 2 - 4 are repeated until the specified accuracy is reached. If iteration convergence conditions are satisfied, then proceed to the next time step.

IV. Results of Computational Experiment

The effects of porosity and permeability of the aquifer and gas injection rate on the dynamics of the fields of temperature, pressure, water and hydrate saturation were studied in computational experiment. Other initial parameters were the following:

$\rho_w = 1000$ kg/m^3, $\rho_s = 2650$ kg/m^3, $\rho_h = 920$ kg/m^3,
$c_w = 4200$ J/(kg·K), $c_s = 700$ J/(kg·K),
$c_h = 3210$ J/(kg·K), $c_g = 2093$ J/(kg·K),
$q = 510000$ J/kg, $\varepsilon = 0.147$, $\mu_w = 1.8 \cdot 10^{-3}$ Pa·s,
$\mu_g = 1.3 \cdot 10^{-5}$ Pa·s, $p_0 = 3.0 \cdot 10^6$ Pa, $T_0 = 274.15$ K,
$T_w = 279.15$ K, $H = 10$ m, $r_b = 0.1$ m, $r_k = 300.1$ m,
$r_{out} = 1000.1$ m, $n = 3000$, $\tau = 100$ s.

Gas constant, critical pressure and temperature, and empirical coefficients in equation (11) were calculated according to the composition of the injected natural gas. It corresponds to the Sredne-Botuobinskoye field in the Republic of Sakha (Yakutia): $CH_4 - 85.90$, $C_2H_6 - 7.32$, $C_3H_8 - 2.24$, $iC_4H_{10} - 0.26$, $nC_4H_{10} - 0.68$, $iC_5H_{12} - 0.17$, $nC_5H_{12} - 0.24$, $C_6H_{14} - 0.08$, $CO_2 - 0.05$, $N_2 - 2.64$, $H_2 - 0.14$, $He - 0.28$ (volume percents); $R = 445.6$ J/(kg·K), $p_c = 4.555$ MPa, $T_c = 204.134$ K, $\alpha_1 = 7.82$ K, $\alpha_2 = 166.64$ K. The field was chosen primarily due to the fact that the experimental data on the equilibrium conditions of hydrate formation are available for its gas, and they were used to calculate empirical coefficients of relation (11).

The computational experiment was carried out to evaluate the role of gas injection flow rate (1 m^3/s and 5 m^3/s) and the different combinations of porosity and permeability of a reservoir (1 – $m = 0.15$, $k = 8 \cdot 10^{-13}$ m^2; 2 – $m = 0.15$, $k = 8 \cdot 10^{-14}$ m^2; 3 – $m = 0.4$, $k = 8 \cdot 10^{-13}$ m^2; 4 – $m = 0.4$, $k = 8 \cdot 10^{-14}$ m^2) in dynamics of hydrate and water saturation fields as well as temperature and pressure ones. Initially the aquifer does not contain hydrates and its water saturation equals 0.9. The most essential results of calculations can be seen at Fig. 1 - 11. Their analysis leads to the following conclusions.

At first, consider dynamics of gas temperature fields because of its determinative role in hydrate formation.

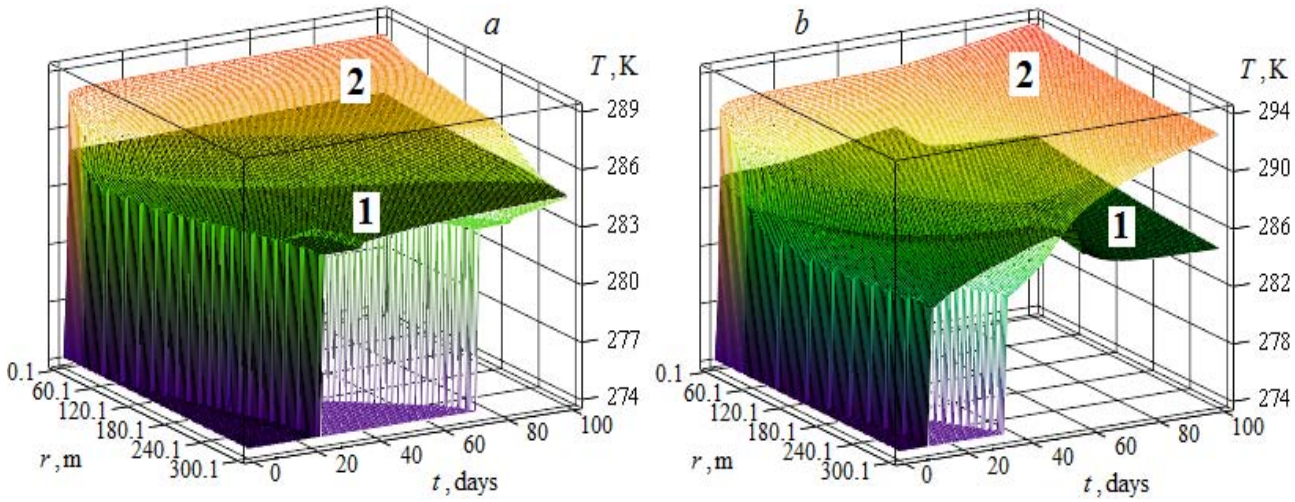

Fig. 1: Dynamics of temperature fields:*a* – mass flow rate equals 1 m^3/s; *b* – mass flow rate equals 5 m^3/s (figures at the surfaces correspond to combinations of porosity and permeability)

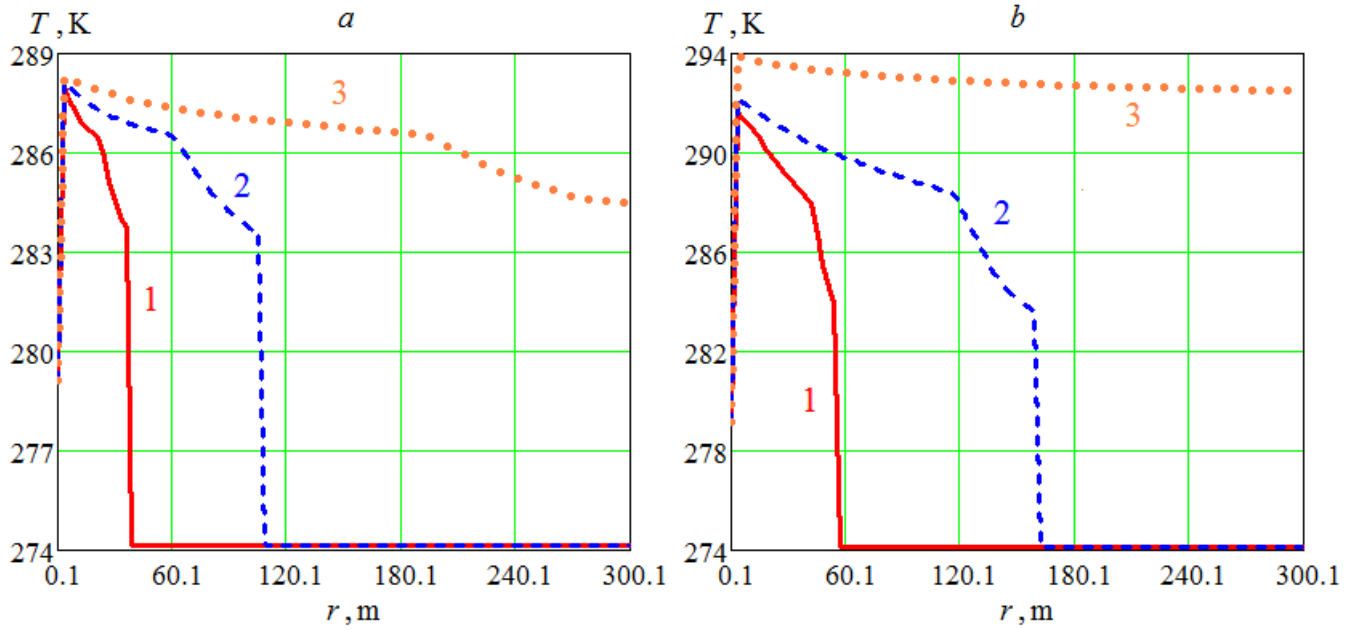

Fig. 2: Temperature distribution in reservoir: *a* – mass flow rate equals 1 m^3/s; *b* – mass flow rate equals 5 m^3/s (1 – t = 1.25 days, 2 – t = 10 days, 3 – t = 100 days)

It is seen from Figures 1 - 3 (Fig. 2 and Fig. 3 correspond to lower permeability) that over a relatively short time interval (several hours) temperature goes up significantly: at high flow rate – about 20 degrees, and about 15 degrees – at low flow rate (cf. curves 1 in Fig. 3*a* and Fig. 3*b*). After 10 days of gas injection, temperature front reaches 110 m and 160 m distances and in 70 and 35 days – reservoir boundary, for low and high injection rate, correspondingly (curves 2 in Fig. 2*a*, 2*b* and curves 3 in Fig. 3*a*, 3*b*). At the end of gas injection for high flow rate the temperature is almost leveled throughout the reservoir (curve 3 in Fig. 2*b*). Figure 1 illustrates all these features and demonstrates an influence of permeability on velocity of temperature front and on temperature dynamics and distribution (cf. surfaces 1 and 2 which correspond to permeability $k = 8 \cdot 10^{-13}$ m^2 and $k = 8 \cdot 10^{-14}$ m^2, correspondingly, with porosity being equal to 0.15).

Permeability value is crucial for pressure dynamics and distribution in the storage (cf. surfaces 1 and 2 in Fig. 4).

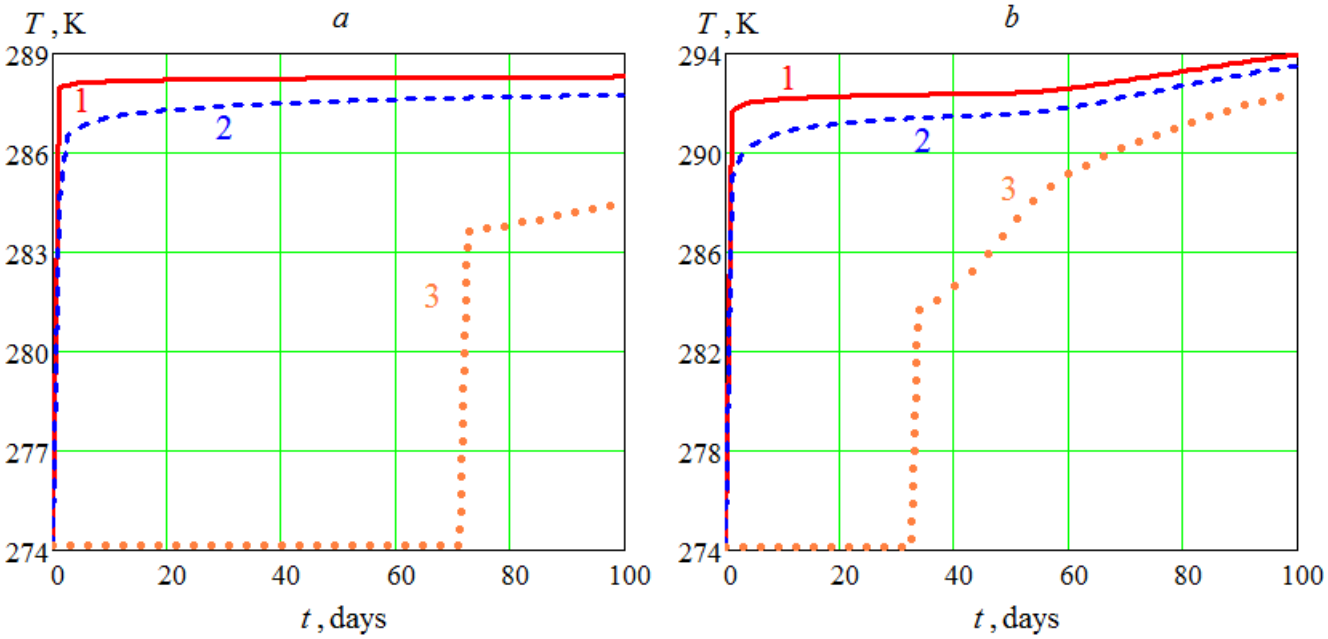

Fig. 3: Temperature dynamics: *a* – mass flow rate equals 1 m^3/s; *b* - mass flow rate equals 5 m^3/s (1 – r = 3.1 m, 2 – r = 30.1 m, 3 – r = 300.1 m)

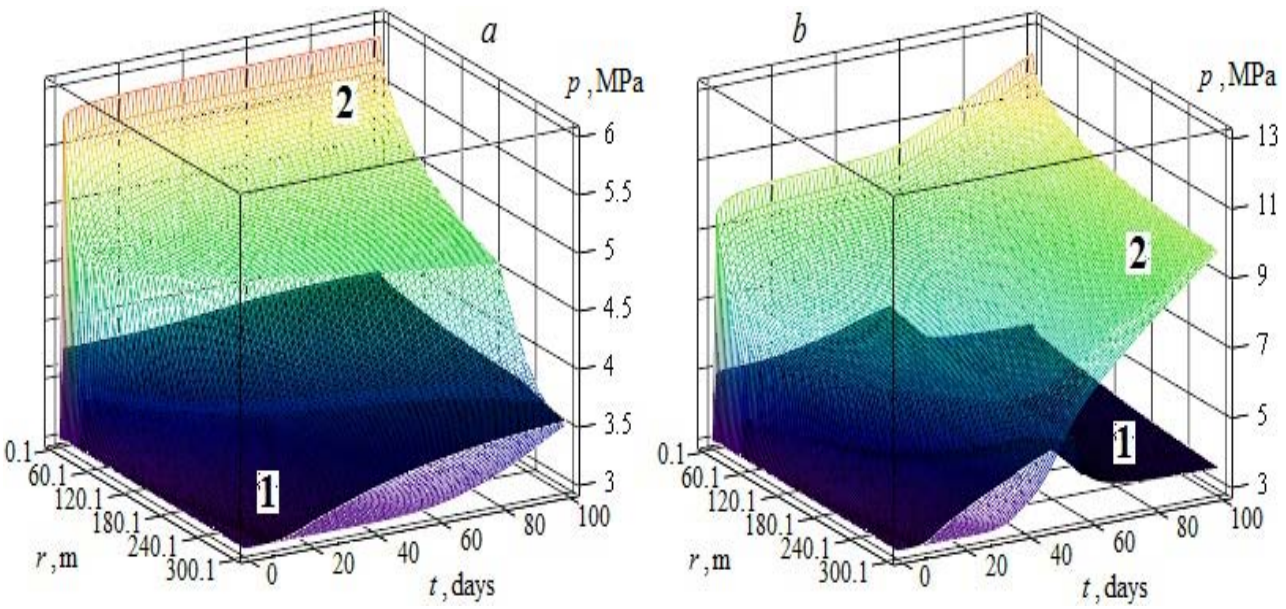

Fig. 4: Dynamics of gas pressure: *a* – mass flow rate equals 1 m /s; *b* – mass flow rate equals 5 m /s (figures at the surfaces correspond to combinations of porosity and permeability)

Near gas well it is growing with the same speed as temperature but at low flow rate it almost reaches its limit of 6 MPa (curve 3 in Fig. 6), while for high flow rate it is growing progressively (curves 1 and 2 in Fig. 6). Pressure growth at high flow rate is twice as much as at low one (cf. Fig. 4*a* and Fig. 4*b* as well as Fig. 5*a* and Fig. 5*b*). For some geological conditions, such high pressure may lead rock fractures.

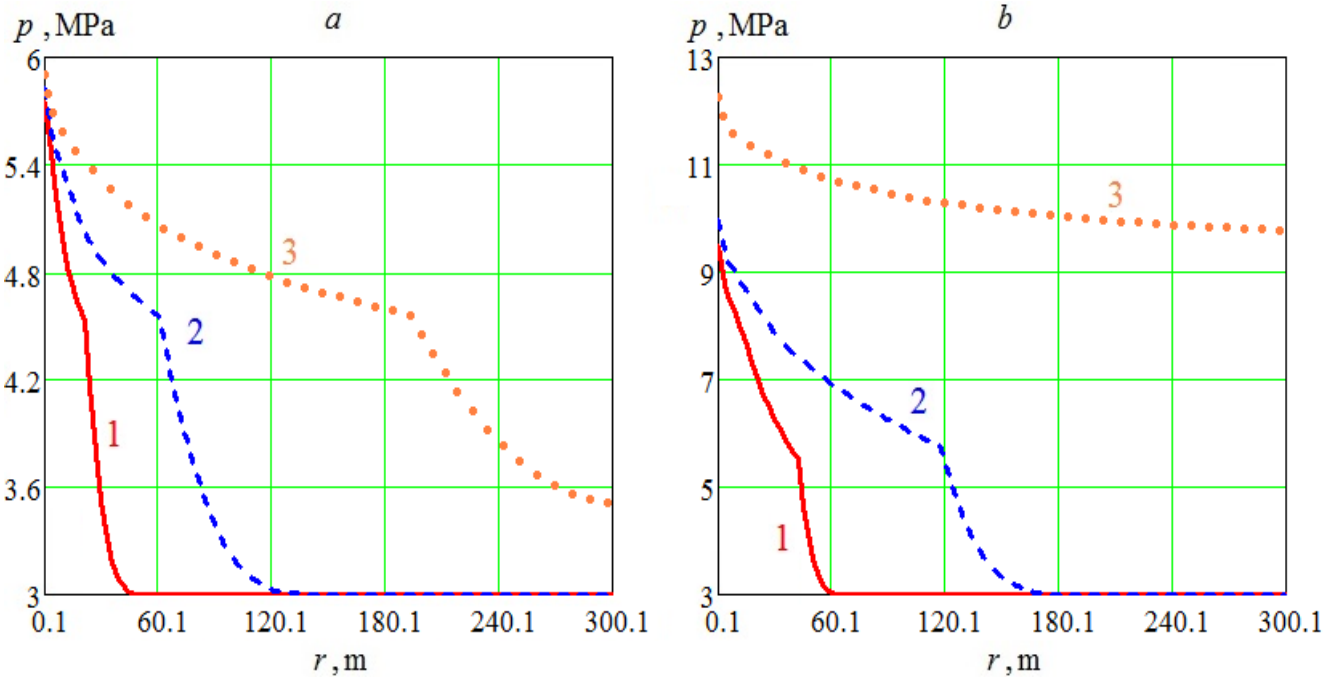

Fig. 5: Pressure distribution in reservoir:*a* – mass flow rate equals 1 m^3/s; *b* – mass flow rate equals 5 m^3/s (1 – t = 1.25 days, 2 – t = 10 days, 3 – t = 100 days)

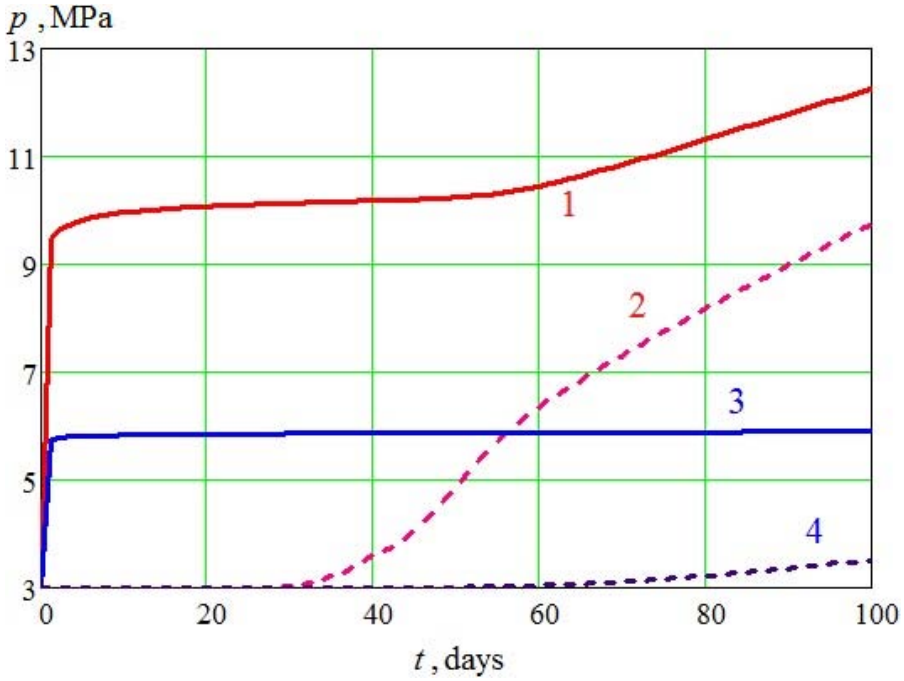

Fig. 6: Pressure dynamics: 1 and 2 – mass flow rate equals 5 m^3/s; 3 and 4 – mass flow rate equals 1 m^3/s (solid lines – r = 0.1 m, dashed lines – r = 300.1 m)

Now consider the influence of dynamics of pressure and temperature fields on water displacement and hydrate formation in the storage. Here we limit the analyses to the case of low permeability because it corresponds to higher temperature and pressure values as can be seen from Fig. 1 and Fig. 4, which may lead to *a priory* unpredictable dynamics of hydrate formation.

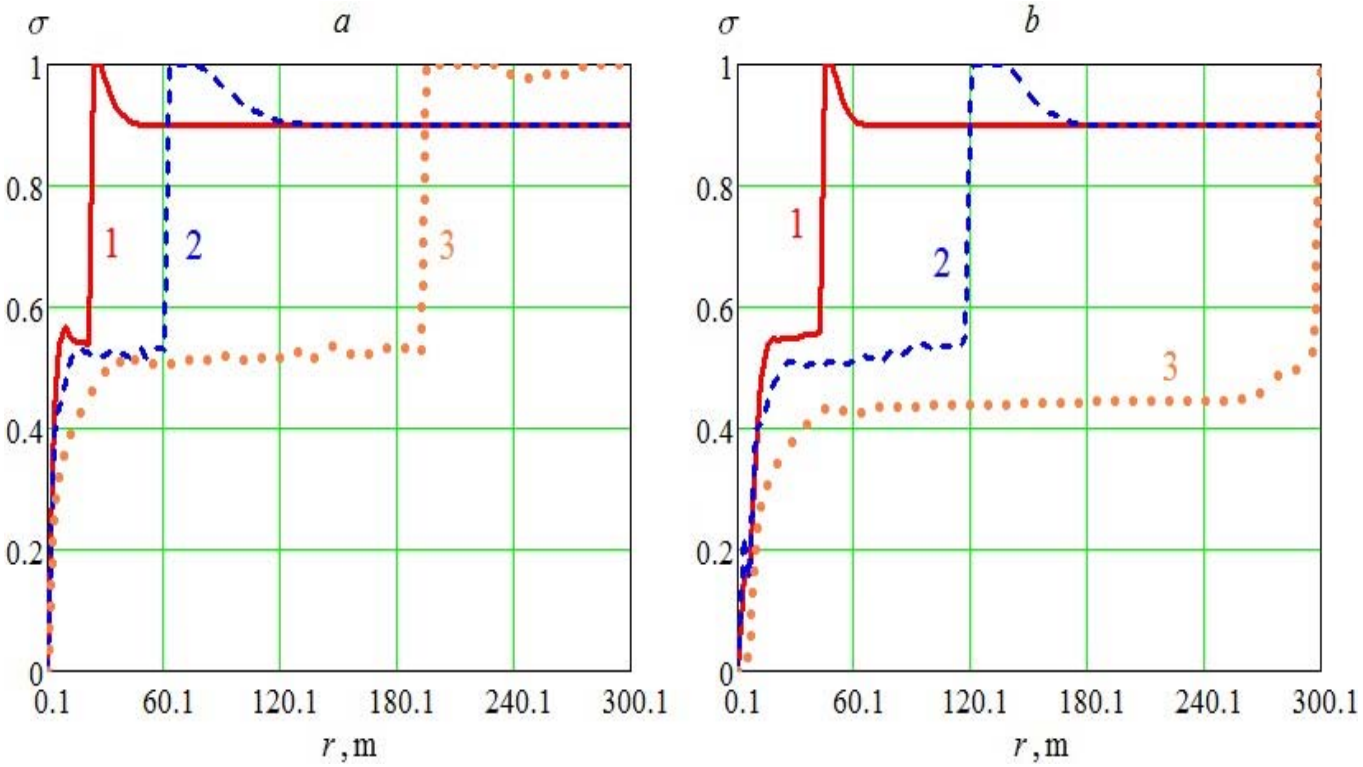

Fig. 7: Water saturation distribution in reservoir:*a* – mass flow rate equals 1 m^3/s; *b* – mass flow rate equals 5 m^3/s (1– t = 1.25 days, 2 – t = 10 days, 3 – t = 100 days)

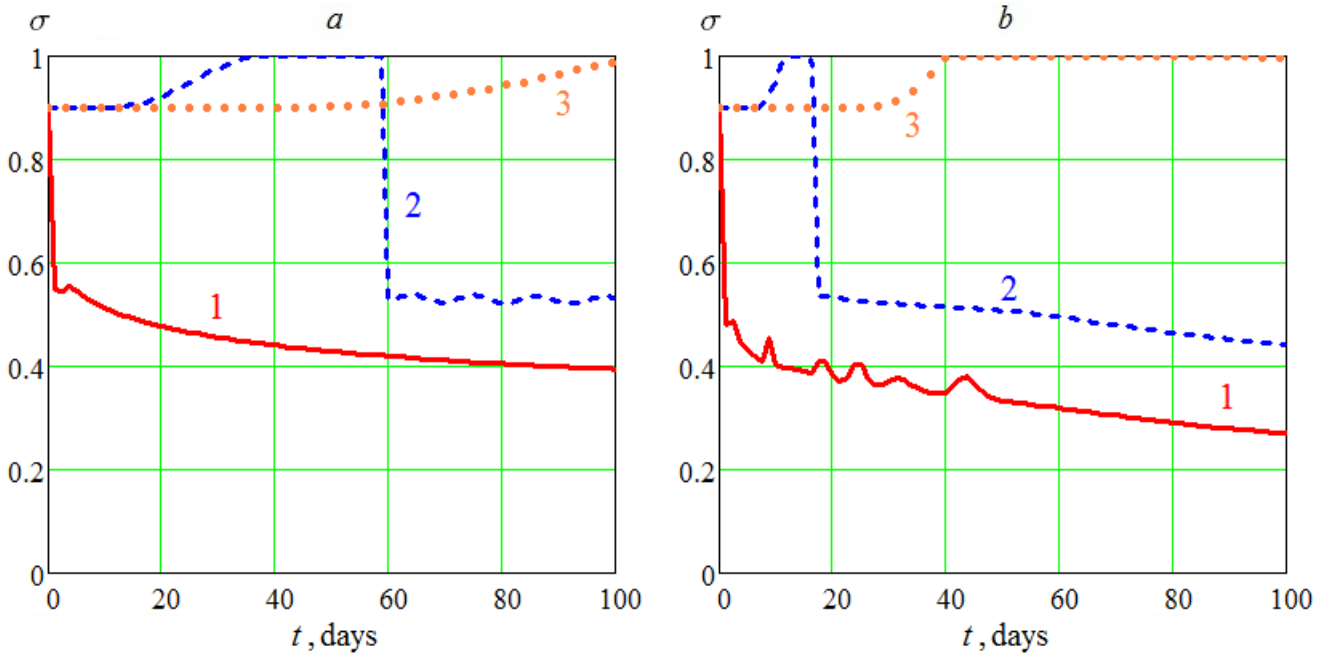

Fig. 8: Water saturation dynamics: *a* – mass flow rate equals 1 m^3/s; *b* – mass flow rate equals 5 m^3/s (1 – r = 12.4 m, 2 – r = 150.1 m, 3 – r = 300.1 m)

Comparison of curves 1 and 2 in Fig. 2 and in Fig. 7 shows that velocity of water saturation front is significantly lower than that of the temperature front. At Fig. 7 and Fig. 8 it is clearly seen that water saturation distribution is in qualitative agreement with the solution of Buckley-Leverett problem [*Charnyi, 1963*]. The effect of hydrate formation, i.e. transition of water into the immobile phase, is manifested in non-monotonic water distribution behind the front and in the fact that water saturation before the front is always lower than 1 (curves 2 in Fig. 8). Naturally, velocity of front propagation is strongly dependent on rate of gas injection. However, in accordance with the theory of two-phase flow in porous media [*Charnyi, 1963*] gas injection cannot displaces all reservoir water (see curve 3 in Fig. 7*b*).

Calculations of hydrate formation show the complicated influence of such competitive factors as reservoir conditions and technology of gas injection.

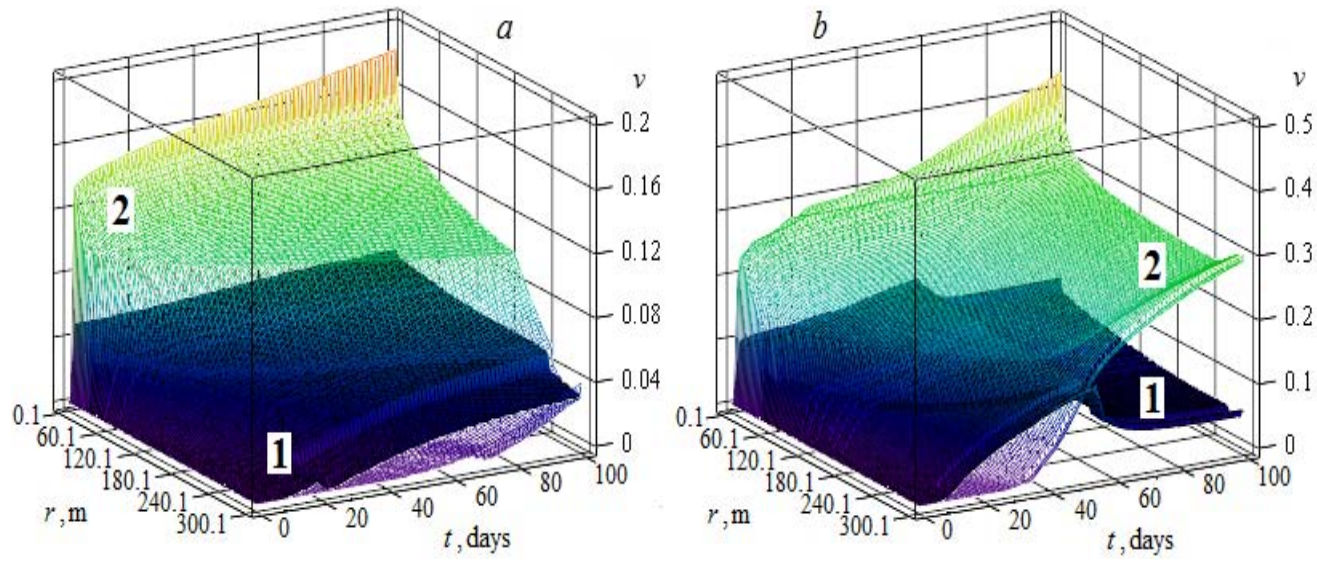

Fig. 9: Dynamics of hydrate saturation: *a* – mass flow rate equals 1 m^3/s; *b* – mass flow rate equals 5 m^3/s (figures at the surfaces correspond to combinations of porosity and permeability)

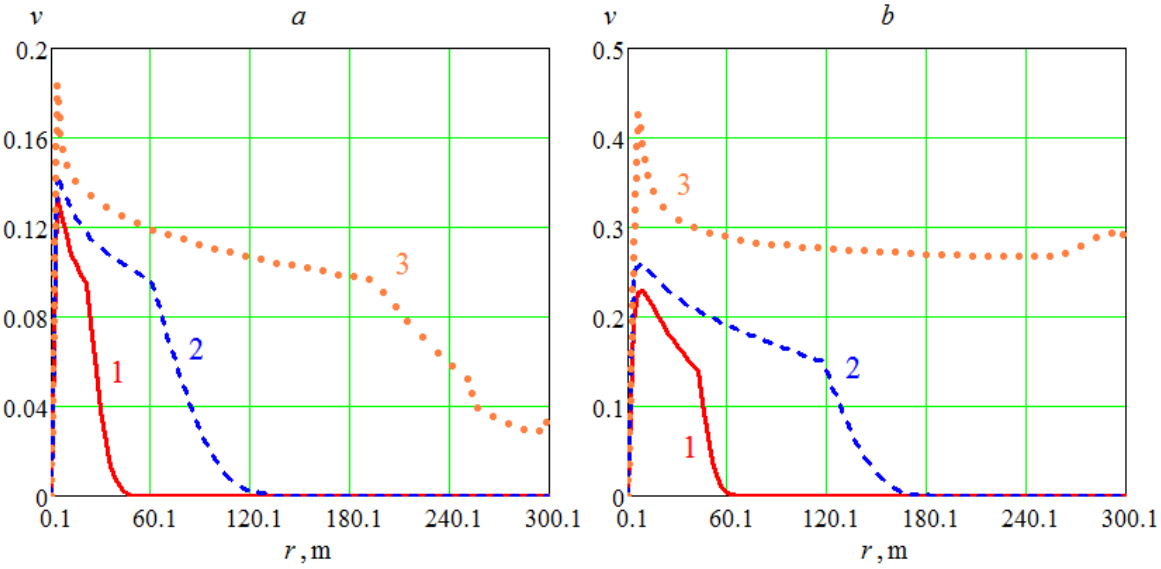

Fig.10: Hydrate saturation distribution in reservoir: *a*– mass flow rate equals 1 m^3/s; *b* – mass flow rate equals 5 m^3/s (1 – t = 1.25 days, 2 – t = 10 days, 3 – t = 100 days)

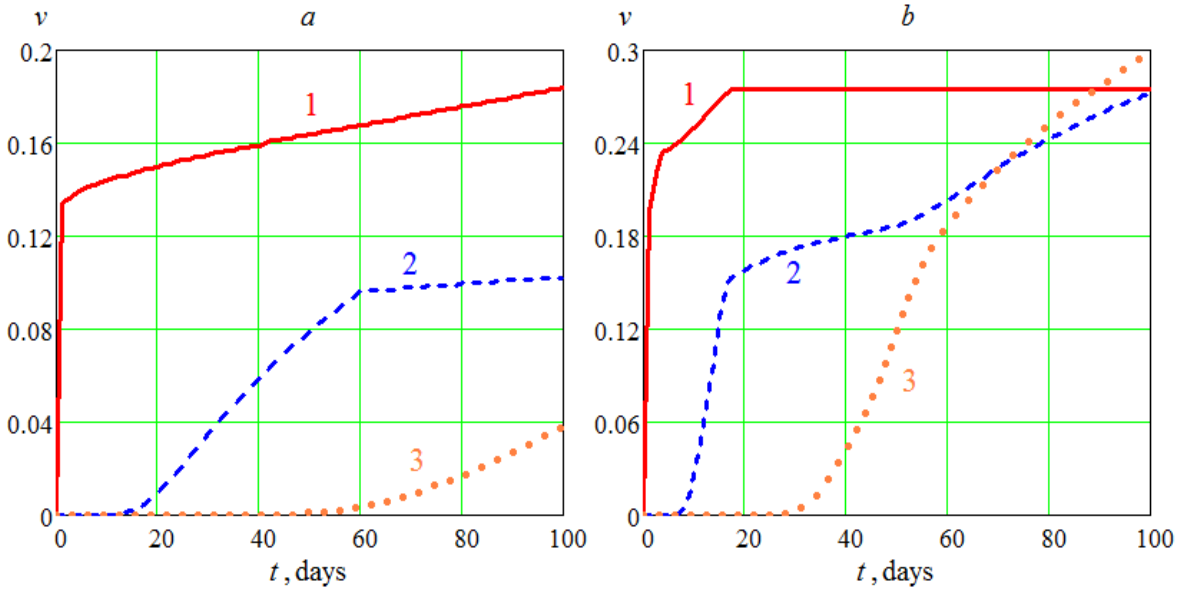

Fig. 11: Hydrate saturation dynamics: *a* – mass flow rate equals 1 m^3/s; *b* - mass flow rate equals 5 m^3/s (1 – r = 12.4 m, 2 – r = 150.1 m, 3 – r = 300.1 m)

First of all, it is seen that higher rate of injection is more favorable for hydrate formation in a reservoir with lower permeability (cf. surfaces 2 in Fig 9*a* and in Fig. 9*b*). It is clear from the fact that high pressure is favorable for hydrate formation. The statement is also supported by comparison of curves 3 in Fig. 10*a* and Fig. 10*b*. Promising is the growth of hydrate saturation at the reservoir boundary with time (curve 3 in Fig. 11*b*).

V. Conclusion

The results of computational experiment show that underground gas hydrate storage development in the subpermafrost aquifers requires a careful analysis of the reservoir geological characteristics and well test data. Specifically, reservoirs with porosity less than 0.2 should be preferred because it ensures a uniform filling of the storage by hydrate. Permeability higher than 10^{-14} m^2 is advantageous to prevent development of excessive pressure at high rate of gas injection, which may result in loss of sealing properties of the reservoir top and bottom.

Additional research is needed to estimate thermal interaction of gas storages with the surrounding rocks and hydrate formation after an injection period.

The results of numerical experiment and proposed mathematical model can be used in the development of scientific bases substantiation of and a basis for technologies of underground hydrate storage of natural gas, as well as toxic gases.

References Références Referencias

1. Balobaev, V.T., Ivanova, L.D., Nikitina, N.M., et al. (2003). Underground Waters of Central Yakutia and the Prospects of their Use. SO RAN, fil. “Geo”, Novosibirsk, 137 pp. (in Russian)
2. Basniyev, K.S., Vlasov, A.M., Kochina, I.N., Maksimov, V.M. (1986). Underground Hydraulics. Nedra, Moscow, 303 pp. (in Russian)
3. Bondarev, E.A., Argunova, K.K., Rozhin, I.I. (2009). Plane-parallel Nonisothermal Filtraton of Gas: the Role of Heat Transfer. J. Eng. Phys and Thermophys. 82 (6), 1059-1065.
4. Bondarev, E.A., Babe, G.D., Groisman, A.G., Kanibolotskii, M.A. (1976). Mechanics of Gas Hydrate Formation in Gas Flows. Nauka, Novosibirsk, 157 pp. (in Russian)
5. Bondarev, E.A., Popov, V.V. (2002). Dynamics of Hydrate Formation at Natural Gas Recovery. Vychislit. Tekhnologii, No. 1, 28-33. (in Russian)
6. Bondarev, E.A., Rozhin, I.I., Popov, V.V., Argunova, K.K. (2015). Assessment of Possibility of Natural Gas Hydrates Underground Storage in Permafrost Regions. Earth's Cryosphere, XIX (4), 64-74.
7. Charnyi, A.I. (1963). Underground Hydrogasdynamics. Gostoptekhizdat, Moscow, 396 pp. (in Russian).
8. Duchkov, A.D., Sokolova, L.S., Ayunov, D.E., Permyakov, M.E. (2009). Estimation of Potential Carbon Dioxide Storage in the Permafrost Regions of Western Siberia. Earth's Cryosphere, XIII (4), 62-68.
9. Istomin, V.A., Kvon V.G. (2004). Prevention and Elimination of Gas Hydrates in Gas Production Systems. IRTs Gazprom, Moscow, 508 pp. (in Russian)
10. Kay, W.B. (1936). Density of Hydrocarbon Gases and Vapors at High Temperature and Pressures. Industr. & Eng. Chem. Res., Vol. 28, pp. 1014-1019.
11. Latonov, V.V., Gurevich, G.R. (1969). Calculation of Natural Gas Compressibility Factor. Gaz. Prom-t, No. 2, 7-9. (in Russian)
12. Sloan, E.D., Koh, C.A. (2008). Clathrate Hydrates of Natural Gases. Taylor & Francis Group/CRC Press, Boca Raton, USA, 720 pp.
13. Vasiliev, V.I., Popov, V.V., Timofeeva, T.S. (2000). Computational Methods in Oil and Gas Fields Development. Izd. SO RAN, Novosibirsk, 126 pp. (in Russian)